NRIAG Journal of Astronomy and Geophysics (2013) 2, 203–211

National Research Institute of Astronomy and Geophysics

NRIAG Journal of Astronomy and Geophysics

www.elsevier.com/locate/nrjag

Parameterization of 18th January 2011 earthquake in Dalbadin Region, Southwest Pakistan

Shafiq-Ur-Rehman [a], Tahir Azeem [b], Abd el-aziz Khairy Abd el-aal [c,*], Asma Nasir [d]

[a] National Seismic Monitoring Center, Pakistan Meteorological Department, Islamabad, Pakistan
[b] School of Geophysics, China University of Geosciences, Haidian District, Beijing, China
[c] National Research Institutes of Astronomy and Geophysics, Helwan, Cairo, Egypt
[d] Department for Geodynamics and Sedimentology, University of Vienna, Austria

Received 2 January 2013; revised 3 June 2013; accepted 4 June 2013
Available online 6 July 2013

KEYWORDS
Balochistan earthquake;
Relocation;
Focal mechanism;
Travel times

Abstract An earthquake of magnitude 7.3 Mw occurred on 18th January 2011 in Southwestern Pakistan, Baluchistan province (Dalbadin Region). The area has complex tectonics due to interaction of Indian, Eurasian and Arabian plates. Both thrust and strike slip earthquakes are dominant in this region with minor, localized normal faulting events. This earthquake under consideration (Dalbadin Earthquake) posed constraints in depth and focal parameters due to lack of data for evaluation of parameters from Pakistan, Iran or Afghanistan region. Normal faulting mechanism has been proposed by many researchers for this earthquake.

In the present study the earthquake was relocated using the technique of travel time residuals. Relocated coordinates and depth were utilized to calculate the focal mechanism solution with outcome of a dominant strike slip mechanism, which is contrary to normal faulting. Relocated coordinates and resulting mechanism are more reliable than many reporting agencies as evaluation in this study is augmented by data from local seismic monitoring network of Pakistan. The tectonics in the area is governed by active subduction along the Makran Subduction Zone. This particular earthquake has strike slip mechanism due to breaking of subducting oceanic plate. This earthquake is located where oceanic lithosphere is subducting along with relative movements between Lut and Helmand blocks. Magnitude of this event i.e. Mw = 7.3, re evaluated depth and a previous study of mechanism of earthquake in same region (Shafiq et al., 2011) also supports the strike slip movement.
© 2013 Production and hosting by Elsevier B.V. on behalf of National Research Institute of Astronomy and Geophysics.

* Corresponding author. Tel.: +20 1226030642.
E-mail address: dewaky@yahoo.com (A.K. Abd el-aal).
Peer review under responsibility of National Research Institute of Astronomy and Geophysics.

ELSEVIER Production and hosting by Elsevier

1. Introduction

An earthquake of Moment Magnitude Mw = 7.3 originated in Southwestern Pakistan (Balochistan province) on 18th January 2011 famously known as the Dalbadin earthquake. The National Seismic Monitoring Center of Pakistan

2090-9977 © 2013 Production and hosting by Elsevier B.V. on behalf of National Research Institute of Astronomy and Geophysics.
http://dx.doi.org/10.1016/j.nrjag.2013.06.001

Meteorological Department reported latitude to be 28.78N and longitude 63.88E and depth 100 km for this earthquake (Fig. 1). The epicenter is located in a remote desert area of the country with a very low population density hence no significant damage reports were received.

As per the earthquake data catalog of the Pakistan Meteorological Department the area exhibits a very low level of seismicity with only a few reported earthquakes in the past. The largest reported event is of magnitude 5.3 in 1980 with a depth of 23 km. Present earthquake is unique in terms of its magnitude and location and poses constraints in its parameters. The present study is focusing to determine the correct depth and focal mechanism of this event. In order to evolve the correct parameters earthquakes are first relocated and then the modified depth is utilized for calculation of the focal mechanism.

2. Methodology

In the present study the Grid Search Method (GSM) based on an iterative process using travel time residuals is utilized for relocation of the earthquake in southwestern Pakistan. The process was first developed by Geiger (1910, 1912) commonly known as Geiger's Iterative method. Clifford (1985) made significant enhancements in Geiger's method to incorporate the nonlinear behavior of travel time as a function of source position and hypocenter location (e.g., Abd el-aal, 2010a,b). Sambridge and Kennett (2001) and Oye and Roth (2003) further enhanced the location algorithm. Lee and Baker (2006) developed the direct location program which was used by Kanamori et al. (2010) for the analysis of the historical 1907 Sumatra earthquake. All these describe the algorithm of computation and technical requirements for the implementation of GSM based on travel time residuals for the present study. Whereas Bai et al. (2006) delineated the significance of seismic network for errors in earthquake locations which is later utilized for assuring the accuracy of results. Focal mechanism is calculated by use of the P wave first motion recording using the algorithm defined by Yagi (2010).

The simple robust method for hypocenter determination in the present study using the iterative process in GSM utilizing travel time residuals is based on the following equation in which the iterative process is based on trail hypocenter (28.78N, 63.88E and depth 100 km) as determined by the data management center of the Pakistan Meteorological Department.

$$(O-C)_{ij} = (t_{ij} - To_{oj}) - T_{ij} = (\partial t_{ij}/\partial x_j)dx_j + (\partial t_{ij}/\partial y_j)dy_j + (\partial t_{ij}/\partial z_j)dz_j + dTo_j + ds_i$$

where t_{ij} and T_{ij} are the theoretical arrival times and the calculated travel times of the j-th event at the i-th station, respectively. ds_i is a correction of a station correction at the i-th station. To is the origin time. O is the observed travel time. C is the calculated travel time. dx, dy, dz and dTo are the corrections to the trial hypocenters. Hypocenter convergence is determined by a reduction of the observed and calculated travel times ($O-C$). The IASP91 velocity model (Kennett and Engdahl, 1991) is used in this study. For P-waves at teleseismic distances, the new tables in IASP91 are about 0.7 s slower than the 1968 P-tables (Herrin 1968) and on average about 1.8–1.9 s faster than the Jeffreys and Bullen (1940) tables. As the times for all phases are derived from the same velocity model, there is complete consistency between the travel times for different phases at different distances and different focal depths. The permanence of the process in Eq. (1) depends upon the availability of data and geographical coverage. Factors like trade off between hypocenter location and station coordinates for low-density seismic network, further augmented by heterogeneous earth structure can hinder the process. Hurukawa and Imoto, 1992 developed the Modified Joint Hypocenter

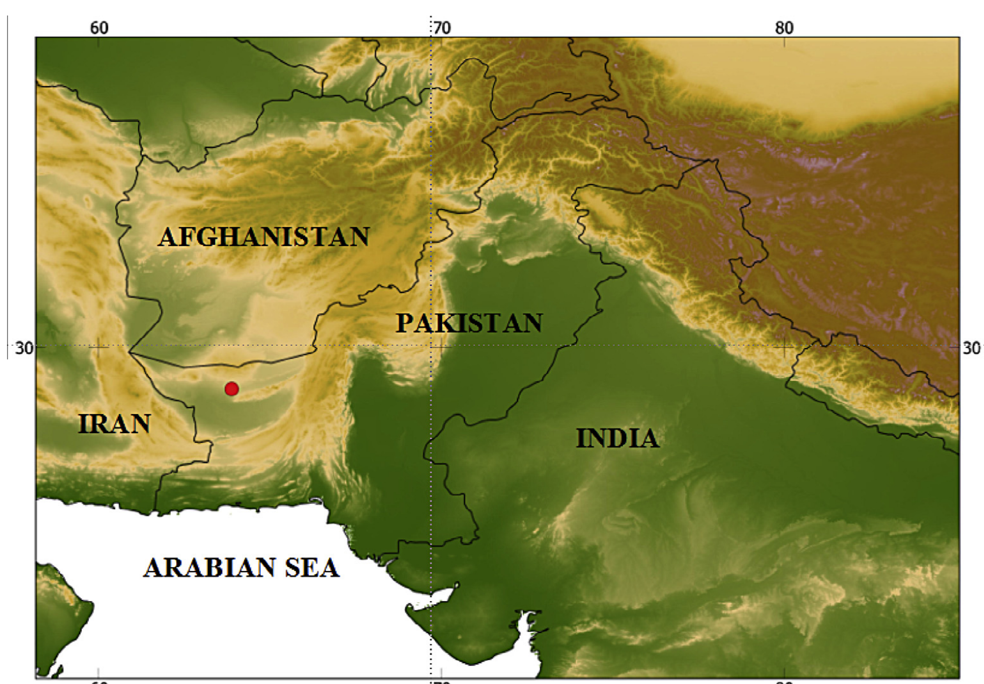

Fig. 1 Map showing the location of Earthquake in Southwest Pakistan. Red circle shows the epicenter.

Determination program (MJHD) to solve this problem of heterogeneous media. For this particular earthquake under consideration only the iterative method with travel time residual was sufficient due to availability of good quality seismic data and good geographic coverage. So MJHD was not adopted for the present study. Further the role of local monitoring network is underscored for the relocation process in this study.

3. Data collection and analysis

For the present study seismic data from PMD and IRIS data centers are utilized. PMD operates a network of ten broad band stations with data communication using satellite technology while eleven short period stations are installed for which data can be obtained manually for desired time. During the analysis of data from local network gaps or breaks in waveform data, high frequency noise and non availability of data from some stations posed serious problems and only five stations from local network were utilized for the present study. The stations include data from five seismic stations (Umerkot, Quetta, Lahore, Muzaffarabad and Islamabad) (Fig. 2). IRIS data management center (IRIS-DMC) provided data from 220 stations (Fig. 2). Out of these 220 stations only 63 stations were selected for the present study based on quality of data.

Seismic Analysis Code (SAC) developed by Lawrence Livermore National Laboratory (LLNL) has been utilized to analyze the seismic data acquired from IRIS and PMD Data centers. Seismogram from each station was analyzed manually to distinguish phase arrivals. In order to incorporate any misjudgments or human errors only one person analyzed all the seismograms. The process is strictly dependent on the availability of good quality seismic data and good geographic coverage (e.g., Abd el-aal, 2010c, 2011, 2012; Abd el-aal and Soliman, 2013).

The analysis was carried out in two steps. At the first step data from IRIS-DMC are analyzed. Due to different delta and geographic coverage data from 63 stations provided clear P wave arrivals. Other stations either lacked data or phase arrival was not clear due to noise. Later in the analysis above mentioned stations of PMD (Fig. 2 blue diamonds) were added to reduce azimuthal gap. PMD stations had a very high noise level and for some stations data were not available having left with only five stations as input for the analysis. All the analyses were performed at both fixed and free depths. In order to obtain the focal Mechanism Solution Fortran program by Yagi (2010) AZMTAK and PMAN are used. These calculate epicentral distances, azimuth and take off angle for computation of lower hemisphere stereographic projection on an equal area net using P wave motion inversion. A total of 58 stations (local and global) were utilized for this study.

4. Results and discussion

At first instance data from only IRIS-DMC stations (Fig. 2) were utilized. Nearest responding stations for the analysis belonged to the Kyrgyz Seismic Telemetry Network (KN) and the Kazakhstan Seismic Network (KZ). IRIS-DMC provided the much needed geographical coverage for the study. Analysis was performed once for fixed depth hypocenter and then for free depth. The RMS values of travel time residuals for fixed depth and free depth analysis are 1.62 and 1.55 respectively. The detailed results of analysis of travel time residual are given in Annex-1 (Table A.1 and Table A.2) in which Table 1 gives the result of relocation of hypocenter at a fixed depth of 30 km

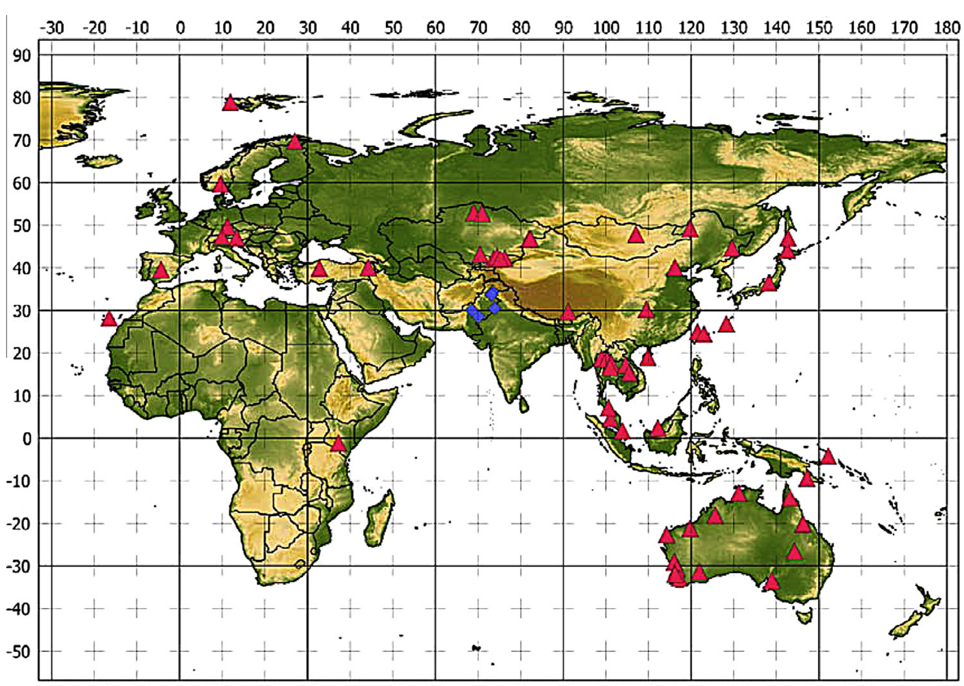

Fig. 2 IRIS-DMC responding stations from different networks. Blue diamonds are PMD stations and Red Triangles are IRIS-DMC Stations.

Table 1 Hypocenter relocation parameters at free depth. Original values of initial trial hypocenter are reported by PMD. Travel time residuals have decreased for joint IRIS-PMD dataset. There is not much change in epicenter position. However there is a considerable decrease in the depth of the focus.

Date	Origin Time UTC	Initial Trial Hypocenter			Relocated hypocenter using IRIS data			Relocated hypocenter using combined (IRIS-PMD) data		
		Lat °N	Long °E	Depth km	Lat °N	Long °E	Depth km	Lat °N	Long °E	Depth km
18-01-2011	20:23:28	28.78	63.88	100	28.73	63.86	75	28.59	63.82	41
RMS of (O-C)					1.55			1.36		

Table 2 Parameters from focal mechanism solution.

Fault Parameters	Strike 1	Dip 1	Rake 1	Strike 2	Dip 2	Rake 2	*P* axis plunge/azimuth	*T* axis plunge/azimuth
	28	88	156	119	66	2	15/76	18/341

while Table 2 gives the results of relocation of hypocenter with free depth analysis using IRIS-DMC data.

In the second phase data from local seismic network from the Pakistan Meteorological Department (PMD) were added. Results of the reevaluated parameters after the inclusion of PMD seismic data are given in Annex-I (Table A.3 and Table A.4) with Table A.3 at fixed depth and Table A.4 at free depth. RMS of residuals after the inclusion of PMD data has decreased with values of 1.58 and 1.36 for fixed and free depth analyses respectively. Results of free depth analysis have shown a general decreasing trend in RMS of observed and calculated travel times supporting more reliable results using free depth location. Table 1 summarizes the results of the analysis.

The data of 63 stations have been used in the study for focal mechanism with inconsistent data from just three stations. One station may have a wrong phase marked which can be attributed to human error. Results of the analysis for focal mechanism are presented in Fig. 3 and Table 2.

United States Geological Survey and Global Centroid Moment Tensor (CMT) have both determined a normal faulting process for this earthquake (Fig. 4 left pane). Results of the present study (Fig. 4 Center Pane) show a dominant strike slip fault movement with a minor component of thrusting. There is no evidence of normal faulting as suspected by many researchers. A previous study by Shafiq et al. (2011) in a nearby region also supports the strike slip movement and points to the fact that non-availability of data can lead to falsified results specially in the case of USGS or CMT solution which does not get any data from this region i.e. Pakistan, Afghanistan, Iran and India. These results have been compared in Fig. 5 showing that inclusion of local data has improved the results.

Bai et al. (2006) used the data at the Northern California Seismic Network (NCSN) and defined errors in locations using data of 117 seismic stations. They have defined the mis-location in earthquake parameters as power law beyond a threshold for stable locations, which is strictly dependent on the number of stations and azimuthal gap (Fig. 5). Based on the findings of Bai et al. (2006) the hypocenter was recalculated in the second phase after the addition of data from the local seismic monitoring network in order to enhance the azimuthal coverage and the number of phases available for analysis and the accuracy and consistency were verified.

In order to judge the accuracy of relocation and focal mechanism analysis, relation between residuals, azimuthal coverage and distance of station was analyzed. For this purpose FORTRAN program DISAZ by Yagi (2010) was utilized. Station distribution in terms of azimuth and distance is shown in Fig. 7, which reveals a cluster of low residual stations up to an azimuthal angle of 150 degrees and a uniform distribution of low residual stations at all distances. Even stations with large azimuthal values and large distance show evenhanded residuals with a maximum value of about 4.0 i.e. only four stations in Fig. 6. These results (Fig. 6) are in agreement with the results of Bai et al. (2006) (Fig. 5) who indicated that the azimuth gap should be below 200 degrees for a reliable location with a minimum of 15 stations to be utilized to reduce errors. Results shown in Fig. 6 satisfy the requirements set forth by Bai et al. (2006) for reducing the location error by provision of data well above the threshold requirement. Amalgamation of PMD and IRIS data has further improved the results and yielded a dominant strike slip mechanism.

Rao and Kalpna, 2005 have presented a tectonic model for the subduction zone between the Indian plate and the Burmese Plate. In the convergence zone between Indian and Burmese

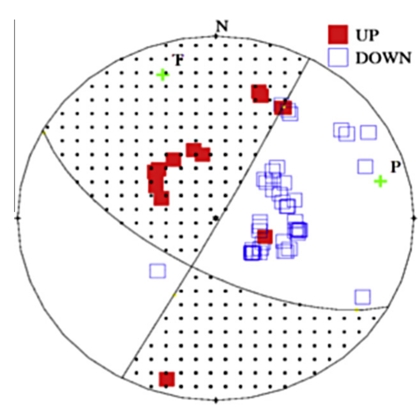

Fig. 3 Focal mechanism solutions of earthquake in Southwest Pakistan. Dominant Strike Slip Component is evident. Compression and dilation are marked by filled and hollow squares.

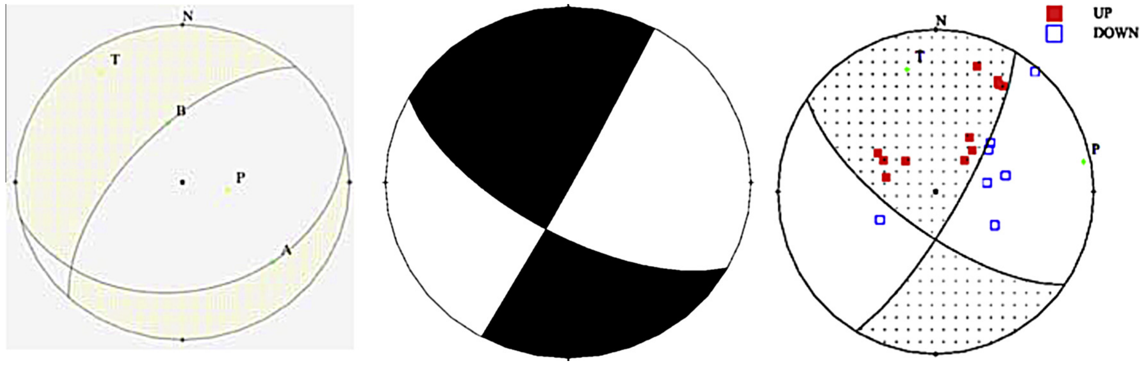

Fig. 4 Focal mechanism solutions of earthquakes in Southwest Pakistan (Left): Harvard Centroid Moment Tensor Solution (CMT) solution for the 18-01-2011 event. (Center): Solution developed for the present study (Right): Earthquake of Mag 5.6 Dated 25-10-2009 reported after (Shafiq et al., 2011).

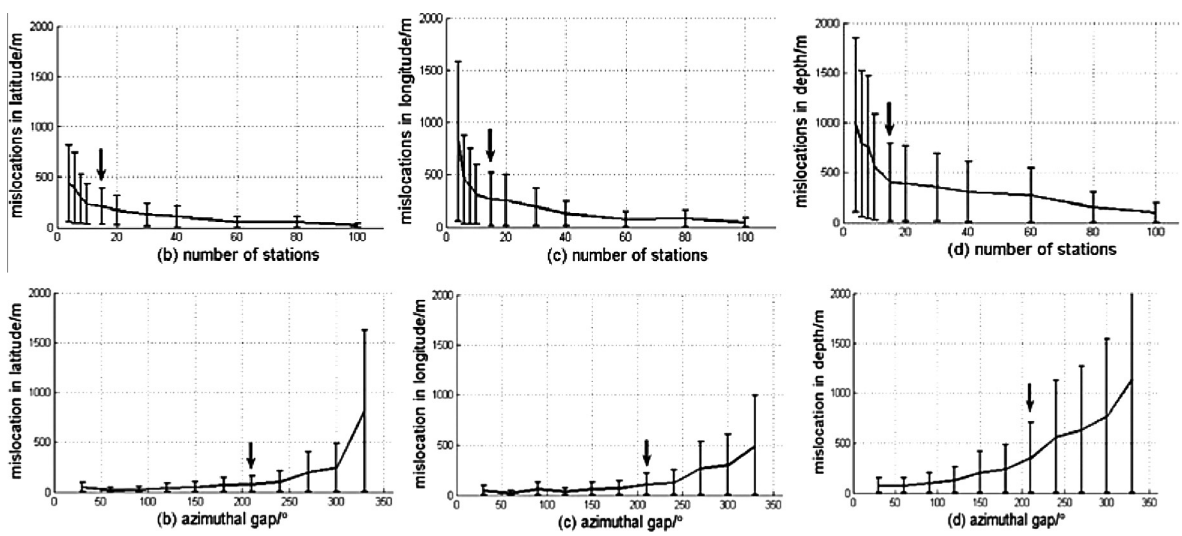

Fig. 5 Mislocation dependent on number of stations (upper pane) and azmimuthal gap (lower pane). Arrows point to threshold of station and azimuth for location error reduction. Source: Bai et al. (2006).

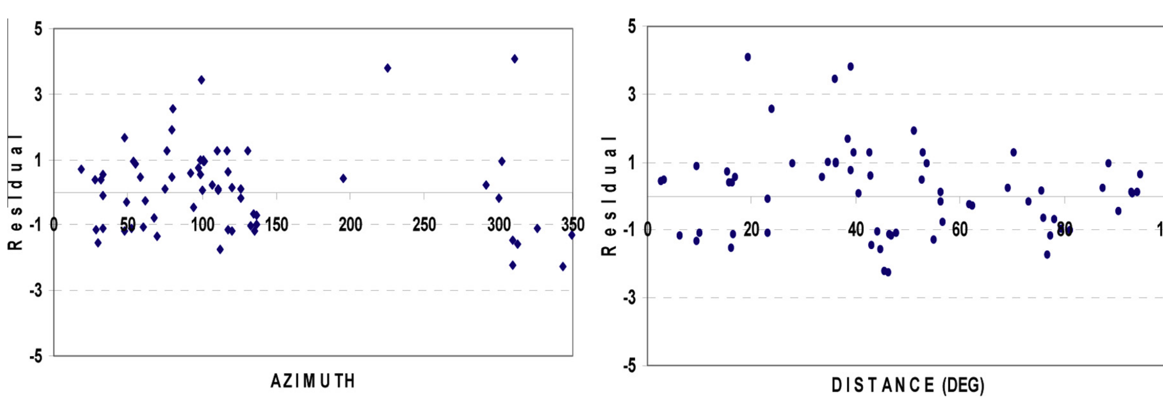

Fig. 6 Distribution of travel time residuals for different azimuthal values and distances.

plates they have suggested strike slip mechanism for the upper 90 km depth and Reverse faulting mechanism for the lower 90 km depth in the subduction zone (Fig. 7). In the present study relocated depth (41 km) of the Balochistan earthquake and focal mechanism (Strike Slip) are supported by the tectonic model of Rao and Kalpna, (2005).

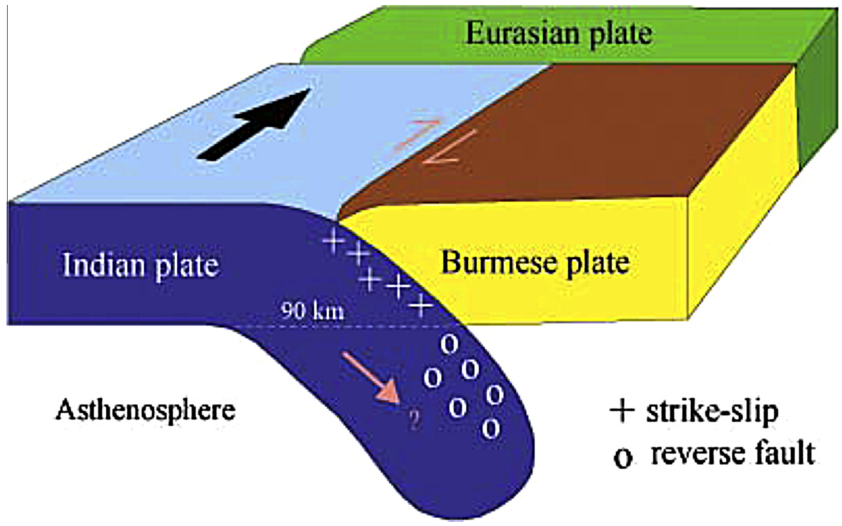

Fig. 7 Source mechanisms of earthquakes at the subduction zone of Indo-Burma ranges Rao and Kalpna, 2005.

5. Conclusion

Earthquakes in the complex tectonic zones of Pakistan pose constraints in their parameters and they are augmented by non-availability of seismic data in and around Pakistan. In the case of earthquake under consideration the earthquake has been relocated twice i.e. with IRIS data first and then location is improved by inclusion of local seismic data from PMD.

The following significant results have been obtained in the present study:

- Present event provided with copious phase counts from global and local seismic networks enabling a reliable depth estimate after the amalgamation of PMD and IRIS data. Relocated hypocenter has a depth of 41 km only in comparison to 100 km depth as reported by PMD.

Table A.1 Parameters after relocation at fixed depth of 30 km.

Hypocenter parameters			Origin time: 20:23:21.1000UTC				Lat:28.59N Long: 63.82E			RMS = 1.62	
Sr. No:	Station Code	Tr. Time	O–C	Sr. No:	Station Code	Tr. Time	O–C	Sr. No:	Station Code	Tr. Time	O–C
1	PBKT	420.73	0.96	26	ARSA	465.96	0.43	51	MORW	703.68	−0.7
2	AML	220.02	0.93	27	QIZ	476.65	0.62	52	BLDU	711.51	−1.28
3	KKAR	216.97	1.12	28	KBA	475.89	−1.43	53	NWAO	722.31	−1.12
4	UCH	223.59	−1.02	29	GRFO	489.81	−1.55	54	MUN	715.54	−0.81
5	AAK	228.02	−0.79	30	BJT	484.73	−1.12	55	KMBL	732.26	−1.15
6	ULHL	235.86	1	31	DAVA	494.05	−2.24	56	COEN	764.85	0.09
7	KZA	228.17	0.75	32	HIA	506.75	−1.18	57	PMG	771	0.8
8	GNI	268.3	4.33	33	KEV	500.19	−2.25	58	HTT	795.48	−0.05
9	MAKZ	303.23	0.02	34	KOM	503.48	−1.16	59	RABL	778.32	−0.67
10	MKAR	303.56	−1.02	35	KONO	513.68	−1.09	60	CTAO	790.71	−0.06
11	LSA	313.53	2.65	36	TATO	542.22	1.89	61	BBOO	784.29	−0.44
12	ZRN	317.83	0.01	37	YOJ	551.81	0.45	62	CTA	790.69	−0.08
13	VOS	318.29	0.02	38	MDJ	560.38	0.85	63	QLP	798.37	0.46
14	ANTO	348.09	1.02	39	SBM	554.1	1.26				
15	CHTO	397.2	0.6	40	KBS	567.79	−1.41	Tr. Time = Travel Time			
16	PHRA	408.39	1.06	41	JOW	578.9	0.08	O−C = Observed – Calculated tr.Time			
17	LOEI	421.99	3.5	42	PAB	577.51	−0.24				
18	ULN	440.37	1.62	43	ASAJ	623.57	−0.58				
19	PBKT	420.69	0.92	44	MAJO	615.44	−0.41				
20	ENH	449.93	1.32	45	YSS	619.91	−0.44				
21	PANO	445.14	0.78	46	MACI	664.17	0.13				
22	KMBO	447.43	3.91	47	GIRL	672.35	1.23				
23	IPM	474.55	1.28	48	MBWA	687.67	−0.29				
24	SKLT	450.53	−7.36	49	FITZ	702.26	0.05				
25	UBPT	457.25	0.1	50	MTN	707.78	−1.87				

Table A.2 Parameters after relocation at free depth (calculated depth 75 km).

Hypocenter Parameters			Origin time: 20:23:26.2000UTC				Lat: 28.73N Long: 63.86E			RMS = 1.55	
Sr. No:	Station Code	Tr. Time	O–C	Sr. No:	Station Code	Tr. Time	O–C	Sr. No:	Station Code	Tr. Time	O–C
1	PBKT	415.63	0.59	26	ARSA	460.86	0.41	51	MORW	698.58	−0.95
2	AML	214.92	−0.08	27	QIZ	471.55	0.46	52	BLDU	706.41	−1.5
3	KKAR	211.87	0.17	28	KBA	470.79	−1.35	53	NWAO	717.21	−1.3
4	UCH	218.49	−1.93	29	GRFO	484.71	−1.37	54	MUN	710.44	−1.01
5	AAK	222.92	−1.5	30	BJT	479.63	−0.63	55	KMBL	727.16	−1.25
6	ULHL	230.76	0.26	31	DAVA	488.95	−2.2	56	COEN	759.75	0.39
7	KZA	223.07	0.03	32	HIA	501.65	−0.57	57	PMG	765.9	1.15
8	GNI	263.2	3.48	33	KEV	495.09	−1.65	58	HTT	790.38	0.05
9	MAKZ	298.13	0.3	34	KOM	498.38	−1.73	59	RABL	773.22	−0.21
10	MKAR	298.46	−0.76	35	KONO	508.58	−0.71	60	CTAO	785.61	0.22
11	LSA	308.43	2.45	36	TATO	537.12	2.09	61	BBOO	779.19	−0.35
12	ZRN	312.73	0.65	37	YOJ	546.71	0.75	62	CTA	785.59	0.2
13	VOS	313.19	0.65	38	MDJ	555.28	1.53	63	QLP	793.27	0.66
14	ANTO	342.99	0.71	39	SBM	549	0.97				
15	CHTO	392.1	0.19	40	KBS	562.69	−0.65				
16	PHRA	403.29	0.66	41	JOW	573.8	0.43	Tr. Time = Travel Time			
17	LOEI	416.89	3.12	42	PAB	572.41	−0.18	O–C = Observed – Calculated tr.Time			
18	ULN	435.27	2.13	43	ASAJ	618.47	0.18				
19	PBKT	415.59	0.55	44	MAJO	610.34	0.27				
20	ENH	444.83	1.43	45	YSS	614.81	0.32				
21	PANO	440.04	0.46	46	MACI	659.07	0.3				
22	KMBO	442.33	2.34	47	GIRL	667.25	0.87				
23	IPM	469.45	0.62	48	MBWA	682.57	−0.47				
24	SKLT	445.43	−7.97	49	FITZ	697.16	−0.03				
25	UBPT	452.15	−0.18	50	MTN	702.68	−1.76				

Table A.3 Parameters after relocation at a fixed depth of 30 km (PMD-IRIS data).

Hypocenter Parameters			Origin time: 20:23:26.2000UTC				Lat: 28.59N Long: 63.79E			RMS = 1.58	
Sr. No:	Station Code	Tr. Time	O–C	Sr. No:	Station Code	Tr. Time	O–C	Sr. No:	Station Code	Tr. Time	O–C
1	UMKT	88.79	−0.66	26	PANO	445.14	0.61	51	MACI	664.17	0.25
2	QUET	49.64	1.01	27	KMBO	447.43	3.99	52	GIRL	672.35	1.1
3	LHR	135.26	−0.83	28	IPM	474.55	1.11	53	MBWA	687.67	−0.4
4	MUZF	142.05	−0.62	29	SKLT	450.53	−7.52	54	FITZ	702.26	−0.06
5	ISLM	125.68	1.24	30	UBPT	457.25	−0.06	55	MTN	707.78	−1.98
6	PBKT	420.73	0.78	31	ARSA	465.96	0.51	56	MORW	703.68	−0.81
7	AML	220.02	0.8	32	QIZ	476.65	0.46	57	BLDU	711.51	−1.39
8	KKAR	216.97	1.12	33	KBA	475.89	−1.27	58	NWAO	722.31	−1.17
9	UCH	223.59	−1.15	34	GRFO	489.81	−1.39	59	MUN	715.54	−0.86
10	AAK	228.02	−0.92	35	BJT	484.73	−1.2	60	KMBL	732.26	−1.21
11	ULHL	235.86	0.88	36	DAVA	494.05	−2.16	61	COEN	764.85	−0.01
12	KZA	228.17	0.63	37	HIA	506.75	−1.33	62	PMG	771	0.7
13	GNI	268.3	4.55	38	KEV	500.19	−2.25	63	HTT	795.48	−0.1
14	MAKZ	303.23	−0.08	39	KOM	503.48	−1.32	64	RABL	778.32	−0.76
15	MKAR	303.56	−1.12	40	KONO	513.68	−1.02	65	CTAO	790.71	−0.15
16	LSA	313.53	2.46	41	TATO	542.22	1.74	66	BBOO	784.29	−0.49
17	ZRN	317.83	0.01	42	YOJ	551.81	0.3	67	CTA	790.69	−0.17
18	VOS	318.29	0.02	43	MDJ	560.38	0.77	68	QLP	798.37	0.42
19	ANTO	348.09	1.2	44	SBM	554.1	1.11				
20	CHTO	397.2	0.43	45	KBS	567.79	−1.41				
21	PHRA	408.39	0.89	46	JOW	578.9	−0.06				
22	LOEI	421.99	3.33	47	PAB	577.51	−0.17				
23	ULN	440.37	1.46	48	ASAJ	623.57	−0.71	Tr. Time = Travel Time			
24	PBKT	420.69	0.74	49	MAJO	615.44	−0.47	O–C = Observed – Calculated tr.Time			
25	ENH	449.93	1.15	50	YSS	619.91	−0.5				

Table A.4 Parameters after relocation at free depth using PMD-IRIS data (calculated depth 41 km).

Hypocenter Parameters				Origin time: 20:23:26.2000UTC				Lat: 28.59N Long: 63.82E		RMS = 1.36	
Sr. No:	Station Code	Tr. Time	O–C	Sr. No:	Station Code	Tr. Time	O–C	Sr. No:	Station Code	Tr. Time	O–C
1	UMKT	87.49	−1.19	26	PANO	443.84	0.74	51	MACI	662.87	0.21
2	QUET	48.34	0.45	27	KMBO	446.13	3.79	52	GIRL	671.05	1.25
3	LHR	133.96	−1.34	28	IPM	473.25	1.26	53	MBWA	686.37	−0.19
4	MUZF	140.75	−1.12	29	SKLT	449.23	−7.39	54	FITZ	700.96	0.15
5	ISLM	124.38	0.86	30	UBPT	455.95	0.07	55	MTN	706.48	−1.76
6	PBKT	419.43	0.99	31	ARSA	464.66	0.41	56	MORW	702.38	−0.65
7	AML	218.72	0.39	32	QIZ	475.35	0.6	57	BLDU	710.21	−1.17
8	KKAR	215.67	0.7	33	KBA	474.59	−1.45	58	NWAO	721.01	−1
9	UCH	222.29	−1.53	34	GRFO	488.51	−1.57	59	MUN	714.24	−0.7
10	AAK	226.72	−1.16	35	BJT	483.43	−1.06	60	KMBL	730.96	−1.03
11	ULHL	234.56	0.54	36	DAVA	492.75	−2.24	61	COEN	763.55	0.23
12	KZA	226.87	0.38	37	HIA	505.45	−1.18	62	PMG	769.7	0.94
13	GNI	267	4.07	38	KEV	498.89	−2.26	63	HTT	794.18	0.09
14	MAKZ	301.93	−0.09	39	KOM	502.18	−1.16	64	RABL	777.02	−0.48
15	MKAR	302.26	−1.12	40	KONO	512.38	−1.09	65	CTAO	789.41	0.09
16	LSA	312.23	2.55	41	TATO	540.92	1.91	66	BBOO	782.99	−0.3
17	ZRN	316.53	0.01	42	YOJ	550.51	0.47	67	CTA	789.39	0.07
18	VOS	316.99	0.02	43	MDJ	559.08	0.95	68	QLP	797.07	0.61
19	ANTO	346.79	0.94	44	SBM	552.8	1.28				
20	CHTO	395.9	0.54	45	KBS	566.49	−1.31				
21	PHRA	407.09	1	46	JOW	577.6	0.12				
22	LOEI	420.69	3.45	47	PAB	576.21	−0.2				
23	ULN	439.07	1.67	48	ASAJ	622.27	−0.52	Tr. Time = Travel Time			
24	PBKT	419.39	0.95	49	MAJO	614.14	−0.28	O–C = Observed – Calculated tr.Time			
25	ENH	448.63	1.28	50	YSS	618.61	−0.31				

- There is no evidence of normal faulting in the region. Furthermore normal faulting in the present tectonic framework may not be able to produce such large magnitude earthquakes.
- Mechanism of this earthquake is mainly strike slip with a minor component of thrusting and the present solution is more reliable than the USGS or CMT solution.
- Data from the local seismic network of PMD need to be enhanced for stations' noise levels alongside collaboration in data sharing between different agencies.

Acknowledgments

Authors are thankful to the International Institute of Seismology & Earthquake Engineering (IISEE) Tsukuba, Japan for the provision of knowledge. Furthermore, authors express their gratitude to Mr. Y. Yagi of Tsukuba University for technical assistance in software for P Wave inversion techniques during the Global Seismological Observation Course 2010 at IISEE.

Appendix A.

Tables A.1–A.4.

References

Abd el-aal, A.K., 2010a. Modeling of seismic hazard at the north-eastern part of greater Cairo metropolitan area, Egypt. J. Geophys. Eng. 7, 75–90. http://dx.doi.org/10.1088/1742-2132/7/1/007.

Abd el-aal, A.K., 2010b. Ground motion prediction from nearest seismogenic zones in and around Greater Cairo Area, Egypt. Nat. Hazards Earth Syst. Sci. 10, 1495–1511. http://dx.doi.org/10.5194/nhess-10-1495-2010.

Abd el-aal, A.K., 2010c. Eliminating upper harmonic noise in vibroseis data via numerical simulation. Geophys. J. Int. 181, 1499–1509. http://dx.doi.org/10.1111/j.1365-246X.2010.04594.x.

Abd el-aal, A.K., 2011. Harmonic by harmonic removal technique for improving vibroseis data quality. Geophys. Prospect. 2011 (59), 279–294. http://dx.doi.org/10.1111/j.1365 2478.2010.00918.x.

Abd el-aal, A.K., 2012. Very broadband seismic background noise analysis of permanent good vaulted seismic stations. J. Seismolog. 17 (2), 223–237. http://dx.doi.org/10.1007/s10950-012-9308-5.

Abd el-aal, A.K., Soliman, M.S., 2013. New seismic noise models obtained using very broadband stations. Pure Appl. Geophys., online first, doi 10.1007/s00024-013-0640-7.

Bai, L., Wu, Zhongliang, Zhang, Tianzhong, Kawasaki1, Ichiro, 2006. The effect of distribution of stations upon location error: statistical tests based on the double-difference earthquake location algorithm and the bootstrap method. Earth Planets Space 58, e9–e12.

Thurber, Clifford H., 1985. Nonlinear earthquake location: theory and examples. Bull. Seismol. Soc. Am. 75 (3), 779–790.

Geiger, L., 1910. Herbsetimmung bei Erdbeben aus den Ankunfzeiten. K. Gessell. Wiss. Goett. 4, 331–349.

Geiger, L., 1912. Probability method for the determination of earthquake epicenters from the arrival time only. Bull. St. Louis Univ. 8, 60–71.

Herrin, E., 1968. Seismological tables for P-phases. Bull. Seism. Soc. Am. 60, 461–489.

Kanamori, H., Rivera, Luis, Lee, William H.K., 2010. Historical seismograms for unraveling a mysterious earthquake: the 1907 Sumatra Earthquake. Geophys. J. Int.. http://dx.doi.org/10.1111/j.1365-246X.2010.04731.x.

Hurukawa, N., Imoto, M., 1992. Subducting oceanic crusts of the Philippine sea and pacific plates and weak-zone-normal compression in the Kanto district, Japan. Geophys. J. Int. 109, 639–652.

Jeffreys, H., Bullen, K.E., 1940. Seismological Tables. British Association for the Advancement of Science, London.

Kennett, B.L.N., Engdahl, E.R., 1991. Travel times for global earthquake location and phase identification. Geophys. J. Int. 105 (2), 429–465.

Lee, W.H.K., Baker, L.M., 2006. Development of a direct search software package for locating poorly constrained earthquakes. Seism. Res. Lett. 77, 291–292.

Oye, V., Roth, M., 2003. Automated seismic event location for hydrocarbon reservoirs. Comput. Geosci. 29, 851–863.

Rao, N.P., Kalpna, 2005. Deformation of the subducted Indian lithospheric slab in the Burmese arc. Geophys. Res. Lett. 32, L05301. http://dx.doi.org/10.1029/2004GL022034, 2005.

Sambridge, M., Kennett, B., 2001. Seismic event location: nonlinear inversion using a neighbourhood algorithm. Pure Appl. Geophys. 158, 241–257.

Seismic Analysis Code, 2010. Lawrence Livermore National Labs. Distributed by IRIS. Peter Goldstein, Arthur Snoke and Brian Savage Binaries and source release, June 2010.

Shafiq Ur Rehman, Tahir Azeem, Abd el-aal A.K., 2011. Relocation of earthquakes. In: Pakistan Using Broadband Stations, Journal of Geophysics special issue on 13th General Scientific Meeting October 2010, National Research of Astronomy and Geophysics, Egypt, pp. 2–17.

Yagi, Y., 2010. Source Mechanism, software lecture notes and exercises: Training Course in Global Seismological Observation 2010. International Institute of Seismology and Earthquake Engineering (IISEE), Tsukuba, Japan.